Investigating the origin of AGN X-ray variability through XMM-Newton and WISE data

A. Zaino [1,2], C. Vignali [1,3], P. Severgnini [2], R. Della Ceca [2] and L. Ballo [4]

[1] University of Bologna (DIFA), [2] INAF-OABrera, [3] INAF-OABo, [4] XMM-Newton SOC (ESA)

ABSTRACT

An efficient diagnostic method to find local ($z < 0.1$) Compton-thick AGN consists in selecting sources characterized by hard X-ray colors and low X-ray to mid-IR flux ratio (HR vs. F_X / F_{IR}). This has been done efficiently in the past using 2XMM and IRAS data (Severgnini et al. 2012). I will here summarize my master thesis work, in which I tested the stability of the method outlined above using the latest 3XMM and WISE data, and I investigated its potentialities in finding interesting spectrally variable (including changing-look) XMM-Newton sources.

Diagnostic diagram for AGN classification in the local Universe: HR vs. F_X / F_{IR}

"Threshold" values:

- $\frac{F_X}{\nu_{IR} F_{IR}}$ *<0.02* and *HR4<-0.2*
- $\frac{F_X}{\nu_{IR} F_{IR}}$ *>0.02* and *HR4<-0.2*
- $\frac{F_X}{\nu_{IR} F_{IR}}$ *>0.02* and *HR4>-0.2*
- $\frac{F_X}{\nu_{IR} F_{IR}}$ *<0.02* and *HR4>-0.2*

$$HR4 = \frac{cts\ (4.5\text{-}12\ keV) - cts\ (2\text{-}4.5\ keV)}{cts\ (4.5\text{-}12\ keV) + cts\ (2\text{-}4.5\ keV)}$$

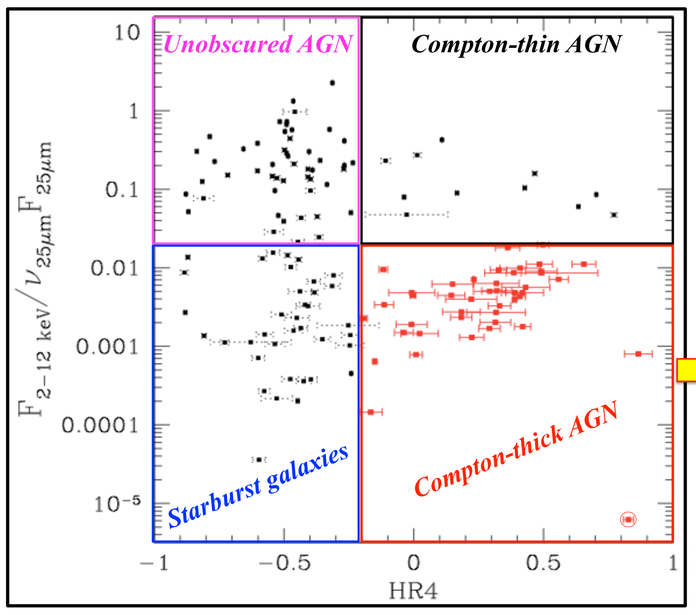

Figure 1. *The X-ray to mid-IR flux ratio vs. hardness ratio diagnostic diagram with 2XMM and IRAS data (Severgnini et al. 2012).*

Original sample: 145 sources obtained cross-correlating the **IRAS PSC** with the **2XMMi-DR2 slim catalogue** (Figure 1)

UPDATING the information (**positions**, **fluxes**, **HR**) of the original sample using the most recent **3XMM-DR5** and **AllWISE source catalog** (see Table1)

THIS WORK: 141 sources* of the original sample

*The exclusion of 4 sources is due to the lack of a WISE detection at 22 μm or to a mismatch between the X-ray and mid-IR emission

Surface density of Compton-thick AGN:
ρ^{CT} ($F_{25\mu m}$>0.5 Jy)~3×10^{-3} src deg^{-2}
(Severgnini et al. 2012)

Table 1. *Comparison between the different catalogues.*

X-ray emission		
	2XMMi-DR2	***3XMM-DR5***
Number of revolutions	*4117*	*7781*
Number of unique sources	*221012*	*396910*
Sky coverage	*420 deg²*	*877 deg²*
IR emission		
	IRAS PSC	***AllWISE***
Number of unique sources	*245889*	*747634026*
PSF (25μm / 22μm)	*1′×5′*	*12″*
Sensitivity (25μm / 22μm)	*650 mJy @10σ*	*2.6 mJy @5σ*

RESULTS

① Stability of the diagnostic diagram in classifying sources considering their average properties

Only 7 sources have shown transitions within the diagram

② Confirmation of the past results (e.g. surface density of CT AGN)

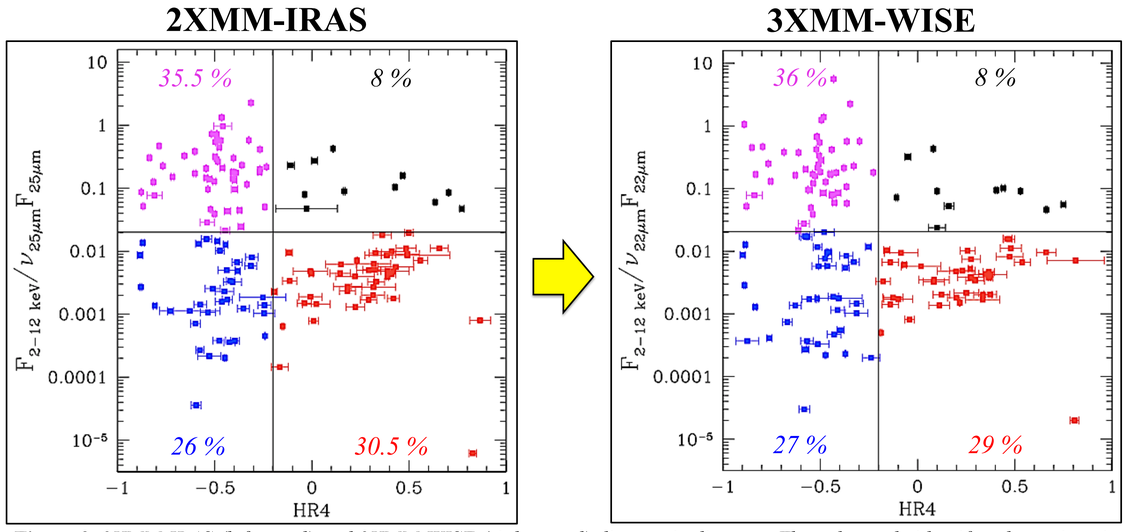

Figure 2. *2XMM-IRAS (left panel) and 3XMM-WISE (right panel) diagnostic diagram. The color code identifies the regions in which the probability to find starburst galaxies (blue symbols), unobscured, Compton-thin and Compton thick AGN (magenta, black and red symbols, respectively) is maximized.*

③ Selection of interesting spectrally variable X-ray sources

The availability of multiple observations in the 3XMM catalogue for ~54% of the sample has allowed us to extend the use of the diagnostic diagram to ***variable AGN*** by plotting individual observations we identified some interesting sources showing transitions between different regions of the diagnostic diagram (i.e. ***changing-look AGN*** – see Figure 3).

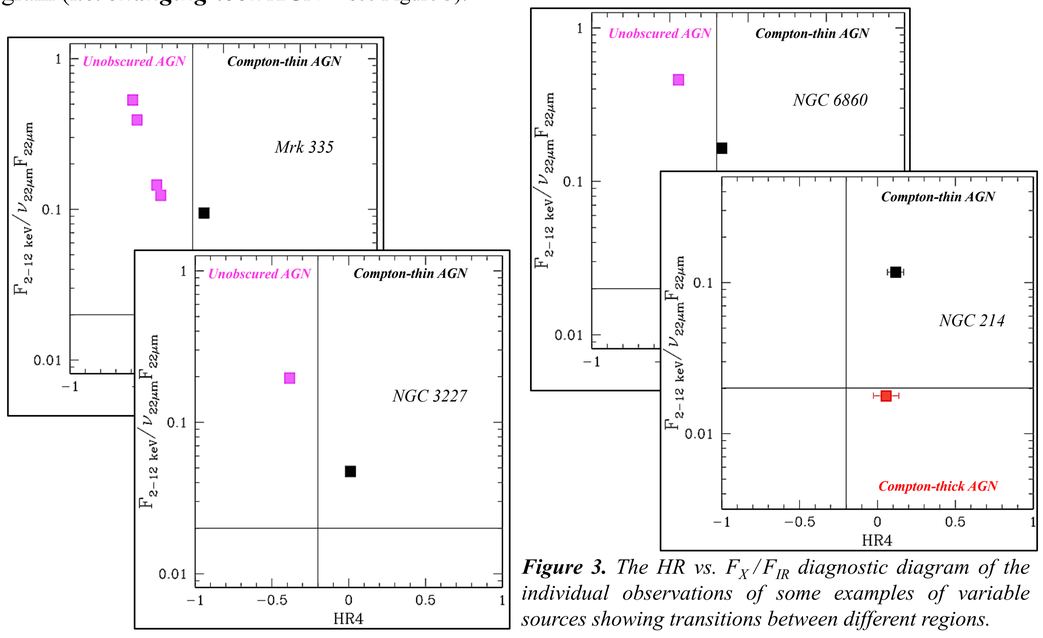

Figure 3. *The HR vs. F_X/F_{IR} diagnostic diagram of the individual observations of some examples of variable sources showing transitions between different regions.*

④ Diagnostic diagram as a tool to have hints on the origin of the observed X-ray variability

➢ **NGC 6860: Seyfert 1/1.5** (Hiroi et al. 2013 / Lípari et al. 1993) **at z=0.015**

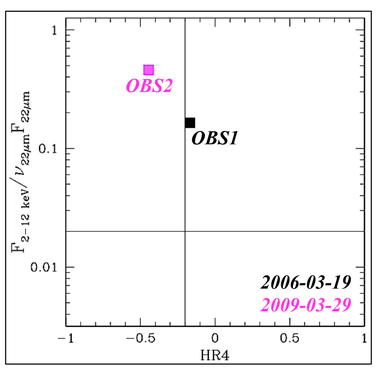

Figure 4. *The HR vs. F_X/F_{IR} diagnostic diagram showing the position of the two observations of NGC 6860.*

HINT: a significant variation in HR points out a ***dramatic change in the column density*** of the neutral gas along the line of sight

CONFIRMED BY SPECTRAL ANALYSIS

X-ray variability driven by the crossing along the line of sight of a neutral cloud covering about 80% of the radiation emitted by the AGN (see Figure 5)

➢ **NGC 4388: Seyfert 2** (Bottacini et al. 2012) **at z=0.00842**

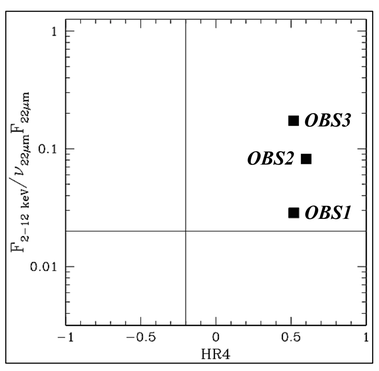

Figure 6. *The HR vs. F_X/F_{IR} diagnostic diagram showing the position of the three observations of NGC 4388.*

HINT: the X-ray variability is due to an ***increasing in the intrinsic emission of the AGN***

CONFIRMED BY SPECTRAL ANALYSIS

Although a little variation in N_H is clearly visible (see Figure 7)**, the main driver of the X-ray variability is a significant increase of the AGN intrinsic emission.**

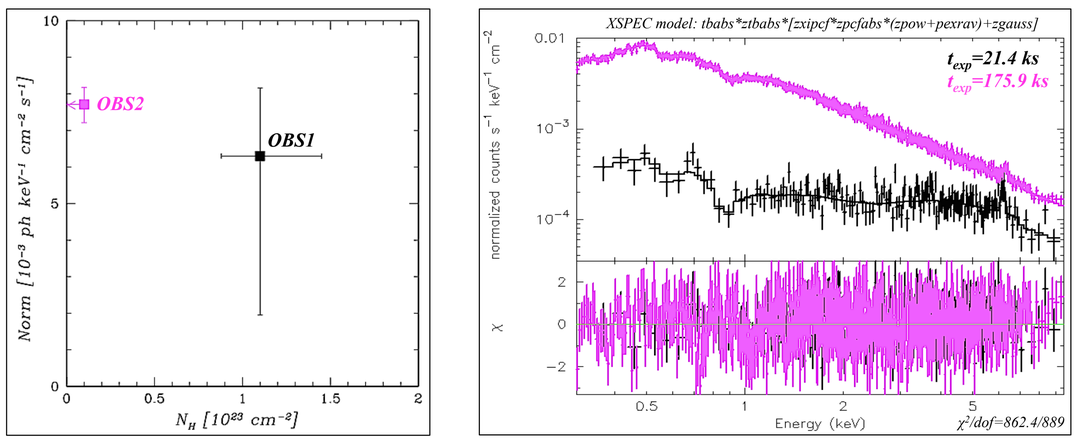

Figure 5. *Values of the neutral gas column density as a function of the normalization of the intrinsic power law in OBS1 and OBS2 (black and magenta square, respectively) of NGC 6860 (left panel) obtained from the X-ray simultaneous fit (right panel).*

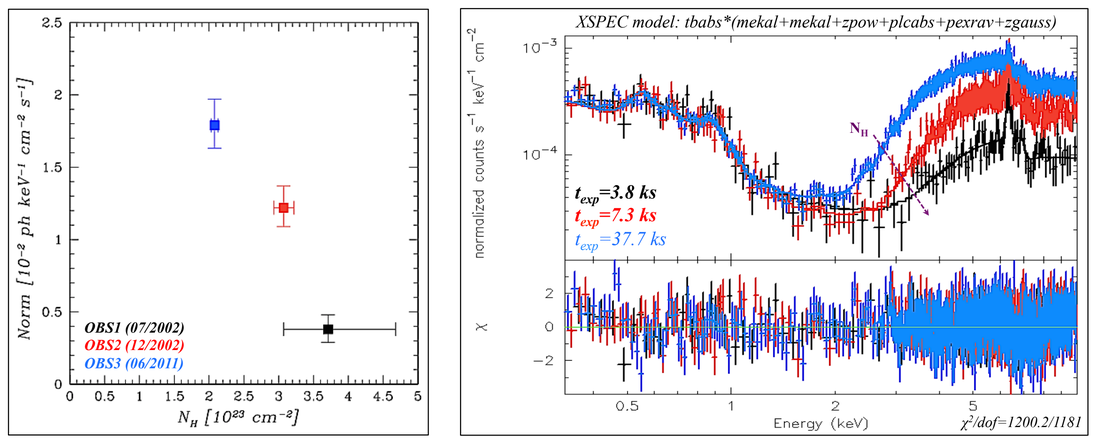

Figure 7. *Values of the neutral gas column density as a function of the normalization of the intrinsic power law in OBS1, OBS2 and OBS3 (black, red and blue square, respectively) of NGC 4388 (left panel) obtained from the X-ray simultaneous fit (right panel).*

Zaino et al. in preparation

References

- Bottacini E., Ajello M. & Grenier J., 2012, ApJS, 201, 34
- Hiroi K., Ueda Y., Hayashida M. et al., 2013, ApJS, 207, 36
- Lípari S., Tsvetanov Z. & Macchetto F., 1993, ApJ, 405, 186
- Severgnini P., Caccianiga A. & Della Ceca R., 2012, A&A, 542, A46